Physical State of Cholesteryl Esters Deposited in Cultured Macrophages†

Julian W. Snow*
Chemistry Department, Philadelphia College of Pharmacy and Science, Philadelphia, Pennsylvania 19104
Holly M. McCloskey, Jane M. Glick, George H. Rothblat, and Michael C. Phillips
Department of Physiology and Biochemistry, The Medical College of Pennsylvania, Philadelphia, Pennsylvania 19129
Received November 17, 1987; Revised Manuscript Received January 15, 1988

ABSTRACT: J774 macrophages load with cholesteryl ester (CE) when incubated with acetylated low-density lipoprotein and cholesterol-rich liposomes; the CE accumulates as cytoplasmic inclusions 1–2 μm in diameter. The CE core of the droplet comprises about 90% of its mass; the predominant CE species present are cholesteryl palmitate (CP, 41%) and cholesteryl oleate (CO, 37%). The thermotropic properties of the inclusions, both in intact cells and after isolation, have been characterized by differential scanning calorimetry. On heating, the inclusions exhibit two endothermic transitions at about 41 and 53 °C with a total enthalpy of 7.7 ± 1.2 cal/g of CE. Very similar thermal behavior is exhibited by a binary mixture containing equal weights of CO and CP; this indicates that these two species dominate the phase behavior of CE in J774 inclusions. A phase diagram for the CO/CP system has been generated, and this reflects simple eutectic behavior. The eutectic is 83% w/w CO, and it melts at 49–50 °C. Below this temperature, CO and CP form two immiscible crystalline phases due to the very limited ability of the unsaturated oleate and saturated palmitate acyl chains to mix in the crystal phase. On heating a 1/1 w/w CO/CP mixture, an isotropic liquid of eutectic composition forms at 49 °C, and the remaining crystalline cholesteryl palmitate melts over the temperature range 50–69 °C. The phase diagram indicates that bulk mixtures of CE molecules in J774 inclusions should be crystalline at 37 °C, the growth temperature of the cells. CO and CP are miscible at all ratios in either the liquid or the liquid-crystalline state where the hydrocarbon chains are melted. The smectic liquid-crystal phase is metastable at all ratios of CO and CP, whereas the cholesteric phase is metastable only in mixtures containing 15–70% and 90–100% CO by weight. These metastable liquid-crystal phases which form on cooling eventually crystallize on storage. The enthalpies associated with the two thermal transitions of the CE in J774 inclusions suggest that the core of this particle comprises microcrystals of CP suspended in a fluid CO-rich phase. The fluid phase could be either metastable, smectic liquid-crystal or metastable, isotropic liquid.

Progression of atherosclerosis involves deposition of cholesteryl ester (CE)[1] in cells of the arterial wall. The cells whose cytoplasms are filled with CE inclusions become the foam cells characteristic of atherosclerotic plaque. Both macrophages (Brown & Goldstein, 1983) and vascular smooth muscle cells (Rosenfeld et al., 1987) can act as precursors of foam cells, and the CE can be deposited in either an ordered or a disordered state (Hata et al., 1974; Small & Shipley, 1974; Katz et al., 1976; Lundberg, 1985). A number of investigators have used various cultured cell systems as models for the study of foam cells; these include macrophages (Brown & Goldstein, 1983), smooth muscle cells (Wolfbauer et al., 1986), and hepatoma cells (Rothblat et al., 1977; Glick et al., 1983; Adelman et al., 1984). The CE stored in macrophages is apparently in a dynamic state, continually being hydrolyzed by a cholesteryl ester hydrolase and reesterified by fatty acyl coenzyme A:cholesterol acyltransferase (Brown et al., 1980). Previous studies in this laboratory have shown that the physical state of the CE in the cytoplasmic droplets can influence the rate of CE clearance from rat hepatoma cells, the CE in ordered, liquid-crystal droplets being hydrolyzed more slowly than that in disordered, liquid droplets (Glick et al., 1983, 1987; Adelman et al., 1984). These experimental results are consistent with the hypothesis that the physical state of lipid in atherosclerotic plaque has a significant effect on the flux of cholesterol between plaque and plasma (Small & Shipley, 1974).

In this paper, we present an investigation of the CE droplets present in the cytoplasm of macrophages. Murine macrophage J774 cells in culture accumulate CE by uptake of complexes of cholesterol-rich liposomes and chemically modified low-density lipoprotein (LDL) (McCloskey et al., 1987) by a scavenger pathway (Brown & Goldstein, 1983). The physical characteristics of the CE inclusions in these cells are likely to be similar to those in the foam cells of atherosclerotic plaque. The composition of the CE molecules deposited in J774 macrophages has been analyzed and the physical state of the inclusions evaluated by using differential scanning calorimetry (DSC). The phase behavior of the CE in the cytoplasmic inclusions is strongly influenced by the thermotropic behavior of the two primary constituents, cholesteryl oleate and cholesteryl palmitate. A phase diagram for this binary mixture is used as the basis for understanding the physical states likely to be adopted by CE present in the cytoplasm of macrophages.

Experimental Procedures

Materials. Cholesterol, cholesteryl esters, triolein, egg phosphatidylcholine, and bovine serum albumin (BSA; fatty

† This work was supported by Program Project Grant HL 22633 and Institutional Training Grant HL 07443.

[1] Abbreviations: acLDL, acetylated low-density lipoprotein; BSA, bovine serum albumin; CE, cholesteryl ester; CO, cholesteryl oleate; CP, cholesteryl palmitate; DSC, differential scanning calorimetry; LDL, low-density lipoprotein; PBS, phosphate-buffered saline; HIFBS, heat-inactivated fetal bovine serum.

0006-2960/88/0427-3640$01.50/0

acid free from fraction V) were purchased from Sigma Chemical Co. (St. Louis, MO). Cholesterol oleate and cholesteryl palmitate were recrystallized from ethanol prior to use in DSC experiments. Coprostanol was purchased from Steraloids Inc. (Wilton, NH). Solvents (ACS grade) were purchased from Fisher Scientific Co. (Philadelphia, PA).

Human low-density lipoprotein (LDL) was prepared from fresh plasma to which 5 mM *N*-ethylmaleimide was added to inhibit lecithin–cholesterol acyltransferase activity (Johnson et al., 1986). Plasma lipoproteins were isolated by sequential density ultracentrifugation (Hatch & Lees, 1968), and LDL was collected between a density of 1.019 and 1.063 g/mL. Acetylated LDL (acLDL) was generated by using acetic anhydride following the method of Goldstein et al. (1979). Modified LDL was examined for its increased electrophoretic mobility using 1% agarose gels (Bio-Rad, Richmond, CA) (Noble, 1968). AcLDL preparations were sterilized by using a 0.45-μm filter before addition to cells.

Cholesterol/Phospholipid Dispersions. Free cholesterol-enriched egg phosphatidylcholine dispersions (liposomes) having molar ratios of free cholesterol/phospholipid greater than 2 were prepared as described by Glick et al. (1983). Dispersions were sterilized by using a 0.45-μm filter before addition to culture media. Aliquots of dispersions were analyzed for free cholesterol and phospholipid contents prior to use.

Cell Culture. J774.1 cells (Ralph et al., 1975), a murine macrophage-like cell line, were grown in T-75 tissue culture flasks on RPMI 1640 medium (Gibco, Grand Island, NY) supplemented with 10% heat-inactivated fetal bovine serum (HIFBS, from Gibco) and 50 μg/mL gentamycin. Cultures were maintained at 37 °C in a humidified, 95% air/5% CO_2 atmosphere. To load J774 cells with CE, the cells were plated at 2.5×10^5 cells/mL in 100-mm petri dishes in 12 mL of RPMI 1640 with 10% HIFBS. Cholesterol-enriched medium was prepared by the addition of cholesterol/egg phosphatidylcholine dispersions plus acLDL (225-μg dispersion of cholesterol/mL and 50 μg of acLDL protein/mL) to RPMI 1640 medium with 1% BSA (McCloskey et al., 1987). RPMI 1640 medium with 1% BSA was used to prepare control cells. All media were incubated overnight at 37 °C prior to use. Cell monolayers grown on 100-mm dishes for 48 h were rinsed 3 times with serum-free medium. Cholesterol-enriched or control medium was added, and the cells were incubated for 3 days at 37 °C. Under these conditions, J774 macrophages accumulated 75–150 μg of esterified cholesterol/mg of cell protein.

For experiments in which whole cell preparations were utilized, CE-loaded cells or control cells were harvested (see below) from four 100-mm dishes. The washed cell pellet was resuspended in 2 mL of phosphate-buffered saline, pH 7.4 (PBS) (Dulbecco & Vogt, 1954), and DSC was performed. Analysis of the cellular free and esterified cholesterol and protein contents was performed on a separate aliquot of the suspension after the cells were disrupted by brief sonication.

Isolation and Analysis of Cholesteryl Ester Inclusions. CE-loaded J774 cells were harvested and pooled from 30 100-mm dishes as follows. The floating population of cells was collected from the tissue culture medium by centrifugation at 1000*g* for 10 min at room temperature. This cell pellet was washed 3 times by repeated suspension and centrifugation in PBS. Cell monolayers were rinsed 4 times with PBS and the cells harvested by gently scraping from the dish into 5 mL of PBS, combined with the harvested floating cells, and pelleted by centrifugation at 1000*g* for 10 min at room temperature. The cell pellet was resuspended in 8 mL of PBS, and the cells were disrupted by sonication for 2 min using the tapered microtip of a Branson 350 sonifier. The disrupted cell suspension was diluted in PBS, pH 7.4, containing 0.25 M sucrose and centrifuged at 45000*g* for 1 h at room temperature in a Beckman SW27 rotor. The floating layer of CE inclusions was collected and washed once by diluting in the PBS/sucrose buffer and recentrifuging under the same conditions. Washed, isolated inclusions were used immediately for DSC analysis or stored in PBS/sucrose buffer with 0.02% sodium azide at 4 °C.

Differential Scanning Calorimetry. DSC experiments with CE-loaded cells or with isolated CE-rich inclusions were conducted on a Microcal MC-1 differential scanning calorimeter (MicroCal Inc., Northampton, MA), using matched 1-mL sample holders. Samples were suspended in PBS (1–5 mg of CE/mL) and scanned at 1 °C/min. An equal volume of PBS was added to the reference sample holder prior to scanning. DSC experiments with lipids extracted from CE-rich inclusions or with mixtures prepared with synthetic lipids were conducted using a Perkin-Elmer DSC-2 differential scanning calorimeter. The samples were scanned against empty sample pans; scanning rates varied from 1.25 to 10 °C/min but were typically 5 °C/min. For such experiments, 1-2 mg of lipid was dissolved in approximately 150 μL of chloroform, and the resulting solution was added in small aliquots to 15-μL aluminum sample pans. Solvent was evaporated under a stream of nitrogen. Prior to being sealed, the pans were placed in a vacuum oven at 40 °C for 2 hours to remove traces of solvent. Enthalpy calibration was achieved with an indium standard; indium and gallium standards were used for temperature calibration.

Analytical Procedures. Lipids were extracted by the method of Bligh and Dyer (1959). Individual lipid classes within the extraction mix were separated by thin-layer chromatography on silica gel G plates (Analtech, Newark, DE) in a solvent system of petroleum ether/ethyl ether/acetic acid (85/15/1 v/v). The isolated CE band was extracted from the silica gel using chloroform/methanol (1/1 v/v), evaporated to dryness under N_2, and stored at −20 °C. Free and esterified cholesterol contents were determined by gas–liquid chromatography using coprostanol as internal standard (Rothblat, 1974). Phospholipid phosphorus content was analyzed by the method of Sokoloff and Rothblat (1972). Triglyceride mass was quantitated by using the PeridoChrom enzymatic/colorimetric kit obtained from Boehringer-Mannheim (Indianapolis, IN). The triglyceride assay was modified to a microassay performed in ELISA microtiter plates. The total assay volume was 175 μL of which 25 μL was triolein standard or unknown sample solubilized in 2-propanol. Fatty acyl groups of cholesteryl esters were analyzed by gas–liquid chromatography after transmethylation using the procedure of Morrison and Smith (1964). Spray reagents, Molybdenum Blue, cupric acetate, and the Purpald set (4-amino-3-hydrazino-5-mercapto-1,2,4-triazole) (Sigma Chemical Co., St. Louis, MO), were used to identify minor lipids after separation using thin-layer chromatography. Protein was determined by a modified Lowry procedure (Markwell et al., 1978).

Results

Lipid Composition of Isolated Inclusions. Under the incubation conditions used in this study, cholesteryl esters accumulate in the cytoplasm of J774 macrophages as discrete lipid droplets of which more than 95% exhibit birefringence under polarizing optics. When examined by light microscopy, the CE droplets have mean diameters in the 1–2-μm range; this is similar to the size observed for inclusions in rat hepa-

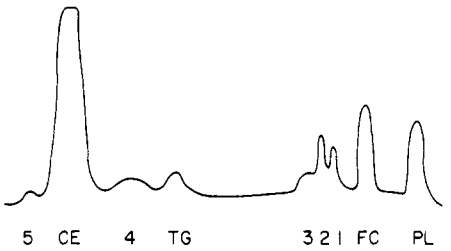

FIGURE 1: Chromatogram of the lipid extract of intracellular cholesteryl ester inclusions isolated from cholesterol-loaded J774 macrophages. The lipids were separated by thin-layer chromatography as described under Experimental Procedures, and the individual lipid bands were visualized by acid staining with 50% sulfuric acid, charred at 110 °C for 15 min, and scanned by densitometry. The thin-layer plate was overloaded with cholesteryl ester in order to detect the minor unknown lipid bands (labeled 1–5). Acid staining of unknown bands 1 and 2 led to the immediate development of a blue color prior to heating. PL, phospholipid; FC, free cholesterol; TG, triglyceride; CE, cholesteryl ester.

Table I: Fatty Acyl Composition of Cholesteryl Esters from Intracellular Lipid Inclusions Isolated from J774 Macrophages

cholesteryl ester fatty acyl group	mol %[a]	cholesteryl ester fatty acyl group	mol %[a]
14:0	4.2 ± 1.9	18:0	7.8 ± 0.8
16:0	41.3 ± 2.0	18:1	36.6 ± 2.1
16:1	5.1 ± 0.6	18:2	4.9 ± 0.7

[a] Mean ± SD of triplicate experiments. The inclusion cholesteryl esters have a saturated/unsaturated fatty acyl ratio of 1.15.

toma cells (Adelman et al., 1984). The lipid composition of the intracellular inclusions isolated from J774 cells shows that 90% of the lipid mass within these particles is CE [CE, 90.1 ± 0.4 wt % (±SD, n = 3)]. Small but significant quantities of free cholesterol, triglyceride, and phospholipid are also associated with the inclusions (free cholesterol, 2.4% ± 0.7%; triglyceride, 2.8% ± 1.3%; phospholipid, 4.9% ± 2.0%). The chromatogram shown in Figure 1 reveals the presence of at least five minor unknown lipid bands (labeled 1–5), in addition to the major lipid classes. Specific stains were used, but negative results were obtained with stains specific for phospholipids and related compounds, prostaglandins, and aldehydes. Spraying with 50% sulfuric acid generated blue coloration in bands 1 and 2 prior to charring. All five minor unknown bands were absent from thin-layer chromatograms of inclusion lipids subjected to saponification by alcoholic KOH. Although their chromatographic behavior suggests that some of these components may be associated with oxidation of CE [cf. Kanazawa et al. (1987)], experiments using radiolabeled CE indicate that none of the minor components originates from CE (data not shown).

Since the macrophage inclusions consist primarily of CE, the fatty acyl composition of the isolated cholesteryl esters was determined (Table I). The predominant CE fatty acyl groups detected were palmitate (16:0) and oleate (18:1) which represented about 41% and 37%, respectively, of the total acyl content. The CE isolated from macrophage inclusions were considerably enriched in the saturated fatty acids compared to isolated cholesteryl esters of cholesterol-loaded Fu5AH rat hepatoma cells (Adelman et al., 1984) and human atheroma (Lundberg, 1985). The saturated/unsaturated fatty acyl ratio for cholesteryl esters isolated from J774 cells was 2-fold higher than that previously reported for the isolated cholesteryl esters from Fu5AH cells (1.15 vs 0.57, respectively). Human atheroma contain a higher percentage of cholesteryl linoleate (Lundberg, 1985) compared to either cholesterol-loaded J774 cells or Fu5AH cells (Adelman et al., 1984). It should be noted that the CE isolated from lipid extracts of human atheroma represent both cellular-derived and extracellular lipoprotein-derived CE. Cholesteryl linoleate is the predominant CE of LDL which has been shown to accumulate within the intima of normal and atherosclerotic arteries (Hoff & Gaubatz, 1982).

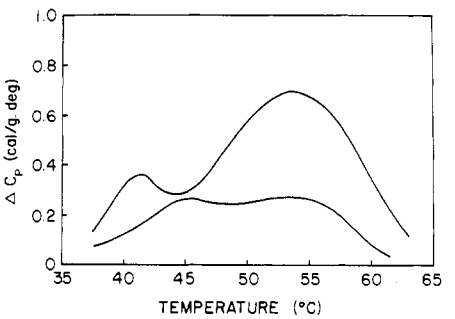

FIGURE 2: Heat capacity curves of J774 macrophages loaded with cholesteryl ester rich inclusions. The upper curve was obtained during the initial heating of the suspension of cells. The lower curve was obtained by cooling to room temperature and rescanning within 1 h.

Thermotropic Properties of Cholesteryl Ester Rich Inclusions. To characterize the phase behavior of the inclusions, DSC experiments were conducted with suspensions of intact J774 cells that were loaded with CE-rich inclusions. Each sample was typically scanned 2 or 3 times, cooling to slightly below room temperature between scans. Figure 2 shows two heat capacity curves obtained during such experiments. The upper curve was obtained from the initial scan, and two peaks with midpoints (T_m) near 41 and 54 °C are apparent. Separate control experiments with cells essentially devoid of CE-rich inclusions showed that the cellular transitions in the temperature range 40–65 °C are similar to, if not identical with, those manifested by the upper curve in Figure 2. It follows that the peaks at 41 and 54 °C in the upper curve are due to cellular structural transitions, such as protein unfolding, as well as phase transitions in the CE inclusions. These transitions were found to be thermally irreversible during subsequent scans of the same sample of cells devoid of CE-rich inclusions. Consequently, the lower curve in Figure 2, obtained by reheating cells loaded with CE inclusions, originates from phase transitions associated with the inclusions. Evidently, the lipid phase transitions are largely reversible under these conditions, since heating the sample a third time resulted in a heat capacity curve very similar to that of the second scan. The two partially resolved peaks in this curve indicate that there are two phase transitions which occur near 45 and 55 °C. The total enthalpy (ΔH) absorbed during these transitions, obtained by determining the area under the two peaks, was 4.9 ± 1.3 cal/g of CE.

DSC experiments were also conducted with inclusions isolated from CE-loaded J774 cells (Figure 3A). This heating profile is qualitatively similar to the lower curve in Figure 2, as expected. Isolated inclusions give rise to clearly resolved transitions with T_m values near 41 and 53 °C. The total enthalpy absorbed during the two transitions is 7.7 ± 1.2 cal/g of CE which is approximately 50% greater than the enthalpy absorbed by the inclusions in the cell suspensions (lower curve, Figure 2). This implies that crystallization of lipid occurred during the isolation procedure (see below). Reheating isolated inclusions resulted in shifts in transition temperature, slight narrowing of peaks, and an increase in enthalpy absorbed during these transitions (data not shown). These results indicate that some structural reorganization occurred subsequent to the initial scan, again indicating that the thermal history of the sample has an important influence on its phase behavior.

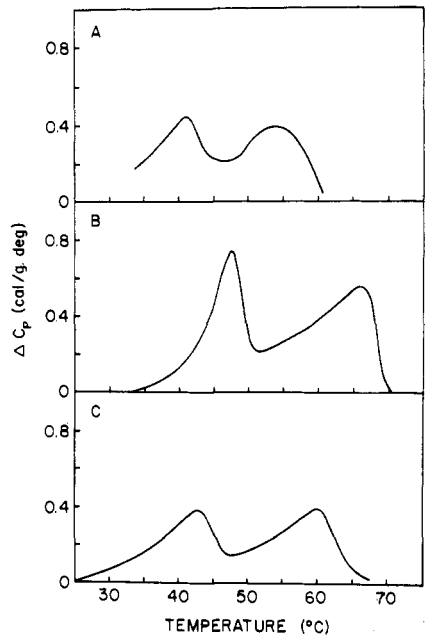

FIGURE 3: Thermotropic behavior of J774 macrophage inclusions and isolated inclusion lipids. (Panel A) Heat capacity curve for cholesteryl ester rich inclusions isolated from J774 cells as described under Experimental Procedures. (Panel B) Heat capacity curve for the total lipid fraction (bulk form) extracted from isolated J774 cell inclusions. The sample was melted and maintained at −20 °C for 20–30 min prior to heating to obtain the profile depicted. (Panel C) Heat capacity curve for the cholesteryl ester fraction (bulk form) extracted from isolated J774 inclusions. The sample was maintained at −20 °C for 20–30 min prior to scanning.

The total lipid and CE fractions were extracted from isolated inclusions and subjected to DSC analysis (Figure 3B,C). The isolated inclusions, total lipid fraction (bulk), and CE fraction (bulk) behave similarly in that they each exhibit two structural transitions between 30 and 70 °C. The transitions observed with the extracted lipid fractions occur at higher temperatures than those observed with isolated inclusions, and they are associated with a greater change in enthalpy. The total lipid fraction exhibits transitions near 47 and 66 °C (ΔH = 10.8 cal/g of total lipid), while the CE fraction undergoes endothermic transitions near 42 and 59 °C (total ΔH = 8.3 cal/g of CE). The T_m and ΔH values for isolated inclusions and the CE fraction are not significantly different, demonstrating that the phase behavior of the inclusions is dominated by the cholesteryl esters. This is not a surprising result since the CE comprises approximately 90% of the total mass of the inclusions.

Figure 4A,B demonstrates the effects of varying the thermal histories of the bulk total lipid and CE fractions from inclusions, respectively. Refrigeration of the samples at −20 °C overnight prior to performing DSC leads to the appearance of an additional endothermic transition at about 39 °C (cf. Figure 3B to Figure 4A and Figure 3C to Figure 4B). There is also an increase in total ΔH so that for the bulk total lipid ΔH = 13.4 cal/g of total lipid and for the CE ΔH = 11.4 cal/g of CE. These two effects are presumably due to a solid–solid transition which does not occur unless the sample is stored at low temperatures for extended periods. This dependence of phase behavior on thermal history is probably a consequence of the slow rate of crystallization of CE and the potential for polymorphism in the crystal state (Small, 1986).

Phase Behavior of Cholesteryl Oleate/Cholesteryl Palmitate Mixtures. Further information regarding the phase behavior of CE-rich inclusions was obtained by preparing mixtures of defined composition using synthetic lipids. Cellular

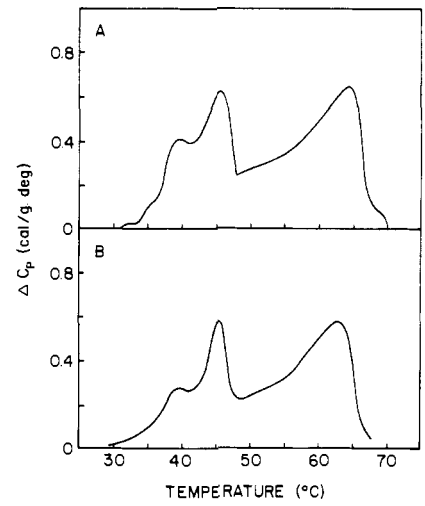

FIGURE 4: Influence of thermal history on the thermotropic behavior of the cholesteryl esters of J774 inclusions. (Panel A) Heat capacity curve for the total lipid fraction (bulk form) extracted from isolated J774 inclusions. The sample was maintained at −20 °C overnight prior to heating to obtain the profile depicted. (Panel B) Heat capacity curve for the cholesteryl ester fraction (bulk form) extracted from isolated J774 inclusions. The sample was refrigerated at −20 °C overnight prior to scanning.

inclusions are complex systems, containing CE with at least six different types of fatty acyl chains, as well as phospholipid, free cholesterol, and triglycerides. The use of model systems allowed us to easily manipulate the composition of the system and therefore to simplify the analysis of the phase behavior. Since cholesteryl esters dominate the thermotropic behavior of inclusions and the predominant CE contained in the inclusions are cholesteryl palmitate (41.3 ± 2.0 mol %) and cholesteryl oleate (36.6 ± 2.1 mol %) (Table I), mixtures of cholesteryl palmitate/cholesteryl oleate were characterized in detail. Three representative heat capacity curves obtained during these experiments are shown in Figure 5. The heating profiles obtained for pure cholesteryl oleate, pure cholesteryl palmitate, and a 50/50 (w/w) mixture of the two [which approximates their ratio in inclusions (Table I)] are depicted in Figure 5A–C. Pure, crystalline cholesteryl oleate and cholesteryl palmitate display sharp melting points near 51 and 80 °C, respectively. The enthalpy of fusion of cholesteryl palmitate (23.4 cal/g) is considerably greater than that of cholesteryl oleate (8.6 cal/g) (Small, 1986). Liquid-crystal transitions are observed in second heating scans (see insets to Figure 5A–C), and the enthalpies associated with these transitions are small, typically on the order of 1 cal/g or less. In each case, the lower temperature peak corresponds to a smectic–cholesteric liquid-crystalline transition and the higher temperature curve to a cholesteric–isotropic liquid transition. The liquid-crystalline transitions for CE can occur at temperatures either below or above crystalline transition temperatures. For example, the smectic–cholesteric and cholesteric–isotropic liquid transitions for pure cholesteryl oleate both occur below 50 °C, whereas the crystalline transition occurs at 51 °C (Figure 5A). Formation of both of these liquid-crystalline phases occurs only by cooling the isotropic liquid. Since they both exist at temperatures below the T_m of the crystalline state, they are metastable, and eventually they will spontaneously revert to the thermodynamically stable crystalline state. In the case of cholesteryl palmitate, the smectic phase is metastable whereas the cholesteric phase is not [the smectic phase crystallizes to a lower melting polymorphic form which reverts almost immediately to the more stable form with T_m near 80 °C (Figure 5B, inset)]. The 1/1

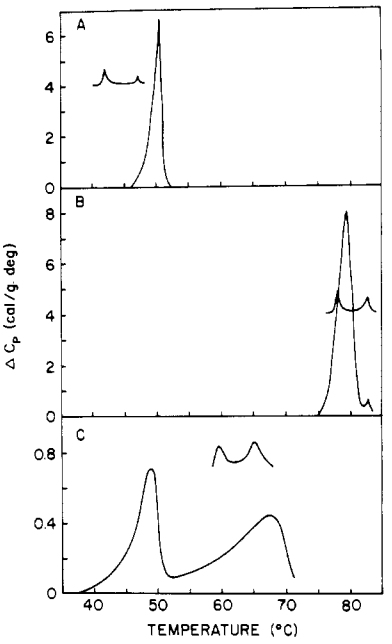

FIGURE 5: Thermotropic behavior of cholesteryl oleate, cholesteryl palmitate, and their mixture. (Panel A) Heat capacity curves for pure cholesteryl oleate. The lower trace with the single large peak corresponds to melting crystalline cholesterol oleate (first heating scan); liquid-crystalline transitions which are apparent in a second heating scan (see text) are represented by the insert curve with the two smaller peaks. (Panel B) Heat capacity curves for pure cholesteryl palmitate showing the crystalline and liquid-crystalline transitions (cf. panel A). (Panel C) Heat capacity curves showing crystalline and liquid-crystalline transitions for a 50/50 (w:w) mixture of cholesteryl oleate/cholesteryl palmitate.

w/w mixture exhibits two endothermic transitions reminiscent of CE inclusions and their lipid extracts (cf. Figure 5C and Figure 3A,C). The transitions in the 1/1 cholesteryl oleate/cholesteryl palmitate mixture occur at somewhat higher temperatures (T_m values of 48 and 67 °C) (Figure 5C) than those exhibited either by isolated inclusions (Figure 3A) or by the CE fraction extracted from the inclusions (Figure 3C) and are somewhat sharper, corresponding to an increased degree of cooperativity. However, the overall thermotropic behavior is qualitatively similar, and the total enthalpy absorbed during the two transitions by the 1/1 w/w cholesteryl oleate/cholesteryl palmitate mixture and isolated inclusions is identical (7.7 cal/g in both cases).

A condensed binary phase diagram (Figure 6) was constructed from data of the type illustrated in Figure 5 using various mixtures of cholesteryl oleate and cholesteryl palmitate. A limited version of the cholesteryl palmitate/cholesteryl oleate phase diagram has been published by Small (1986). This CE mixture is basically a simple eutectic system with a few additional important features. The eutectic point, E (49–50 °C; 83–84% cholesteryl oleate), corresponds to the minimum melting point of any cholesteryl palmitate/cholesteryl oleate mixture and is invariant (three phases coexist at this point). Solidified samples of any other composition will partially melt to form a liquid with the eutectic composition. The remaining solid, either pure cholesteryl oleate or pure cholesteryl palmitate, melts at higher temperatures. Consider, for example, the thermotropic phase behavior of a mixture containing 48% cholesteryl oleate; this composition corresponds to the amount of cholesteryl oleate contained in the inclusions relative to the total amount of cholesteryl oleate and cholesteryl palmitate (Table I). Such a mixture would contain two solid phases of pure cholesteryl palmitate and pure cholesteryl oleate at temperatures below 49–50 °C. At the eutectic temperature,

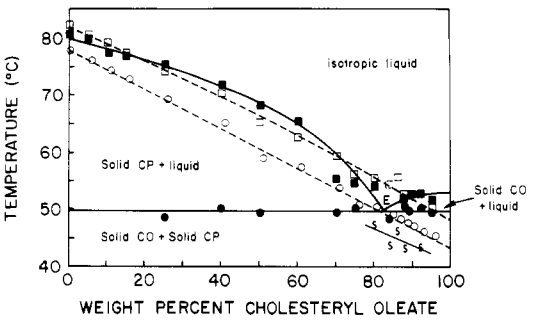

FIGURE 6: Condensed binary phase diagram for cholesteryl palmitate/cholesteryl oleate. The continuous curves representing fits through (●) and (■) were obtained during initial heating scans and represent melting of solid phases of cholesteryl palmitate/cholesteryl oleate to either an isotropic liquid (■) or a liquid of eutectic (E) composition (83–84% cholesterol oleate) (●). The liquid of eutectic composition coexists with either solid cholesteryl palmitate (cholesteryl oleate <83–84%) or solid cholesteryl oleate (cholesteryl oleate >83–84%). The dashed lines representing fits through (○) and (□) were obtained by cooling the samples and reheating before recrystallization occurred. (○) Temperatures of transitions from the smectic liquid-crystalline phase to the cholesteric liquid crystal; (□) temperatures of transitions from the cholesteric liquid-crystalline phase to the isotropic liquid. The points designated s represent a transition between solid solutions. The temperatures are peak temperatures of transitions observed in a Perkin-Elmer DSC-2 at a heating rate of 5 °C/min.

the system would undergo a partial melt to form a liquid phase of eutectic composition (i.e., enriched in cholesteryl oleate). The remaining solid, consisting of pure cholesteryl palmitate, would melt over the temperature range 50–69 °C so that the mixture forms a homogeneous liquid phase at temperatures above about 69 °C. These two endothermic transitions correspond to the lower and higher temperature peaks, respectively, in the DSC scan depicted in Figure 5C.

There are several data points designated as s between 42 and 47 °C in Figure 6 which indicate the existence of another cooperative structural transition over a limited range of composition from approximately 80% to 90% cholesteryl oleate. These correspond to solid–solid transitions, suggesting that a limited amount of cholesteryl palmitate can cocrystallize with cholesteryl oleate (i.e., solid solutions form in this composition range). It is of interest to notice that these transitions occur for samples whose composition is close to the eutectic composition.

Figure 6 should actually be viewed as two separate, superimposed phase diagrams. The dashed lines representing best fits through the data points (○) and (□) were obtained by cooling melted samples and reheating them before recrystallization occurred. These curves correspond to liquid-crystal–liquid-crystal or liquid-crystal–isotropic liquid transitions, as discussed previously. The smectic liquid-crystalline state is metastable at all compositions and is never observed upon melting solid samples. The cholesteric liquid-crystalline state is stable only at cholesteryl oleate compositions between approximately 0–15% and 70–90%.

Discussion

Since the physical state of CE deposits affects their ability to be cleared from the cytoplasm of cells (Glick et al., 1983; Adelman et al., 1984) and presumably from atherosclerotic plaque (Small & Shipley, 1974), it is critical to clarify the factors which control the packing of CE molecules in these deposits. As far as cytoplasmic CE inclusions are concerned, a convenient model of the macrophage-derived foam cell is the J774 cell loaded with cholesterol by incubation with acetylated LDL and cholesterol-rich liposomes. Furthermore, since the present DSC data demonstrate that the two major

CE, cholesteryl oleate and cholesteryl palmitate, dominate the thermotropic behavior of inclusions, this binary CE mixture can be used to derive detailed information about the phase behavior of CE in inclusions.

Phase Behavior of Cholesteryl Oleate and Cholesteryl Palmitate Mixtures. The phase diagram for cholesteryl oleate and cholesteryl palmitate (Figure 6) is consistent with others reported for pairs of saturated and unsaturated CE molecules (Small, 1986). The phase behavior is a consequence of the mixing properties of the saturated palmitate and unsaturated oleate acyl chains. Since unsaturated and saturated hydrocarbon chains do not mix well in the crystalline state, cholesteryl oleate and cholesteryl palmitate crystallize into separate domains at low temperature. Solid solution formation is limited and occurs only in cholesteryl oleate rich mixtures (Figure 6). Similarly, the existence of the cholesteryl oleate rich eutectic is consistent with the general occurrence in CE mixtures of a eutectic rich in the unsaturated component.

The van der Waals attractive interaction energy between saturated hydrocarbon chains is greater than that between unsaturated chains of similar length. Consequently, it is to be expected that cholesteryl palmitate forms a more stable crystalline phase than cholesteryl oleate. The data in Figure 5 support this because cholesteryl palmitate has both a higher melting point and a higher enthalpy of fusion. If either of the pure cholesteryl esters is melted and then cooled, the isotropic liquid is converted into a liquid-crystalline phase. The cholesteric phase of cholesteryl palmitate is stable with respect to the crystal phase whereas the smectic phase eventually crystallizes when held at temperatures below about 75 °C (Figure 5B). In contrast, unsaturated cholesteryl oleate molecules form two metastable liquid-crystal phases (Figure 5A). Mixtures of cholesteryl oleate and cholesteryl palmitate form liquid crystals at all ratios of the two components (Figure 6). Since the melting points of the liquid-crystal states of the CE mixtures fall on the straight line connecting the melting temperatures for the two pure components, it follows that cholesteryl palmitate and cholesteryl oleate are miscible at all stoichiometries when both are in the liquid-crystalline state. This is to be expected because in this situation the oleate and palmitate acyl chains are melted and, although these two hydrocarbon chains do not cocrystallize readily, they are miscible in the fluid state where gauche conformers are stable. The equilibrium phase diagram (Figure 6) indicates that at 37 °C, cholesteryl oleate and cholesteryl palmitate exist as a mixture of crystals of the two components. Before applying this information to interpret CE metabolism in cells, it is necessary to establish how the phase behavior summarized in Figure 6 relates to the condition of cholesteryl esters mixed in inclusions in the cytoplasm of living cells.

Physical State of Cholesteryl Esters in Cells. If the CE in the core of cytoplasmic inclusions in growing cells at 37 °C can adopt its most stable state, then the phase diagram (Figure 6) predicts that an approximately 1/1 w/w cholesteryl oleate/cholesteryl palmitate mixture will be crystalline. Microscopic examination indicates that inclusions in cells are spherical and do not have the needle- or plate-shaped morphology characteristic of CE crystals. Consequently, inclusions must contain some fluid component. Under polarizing optics, the inclusions in J774 cells appear birefringent, indicating that the CE is in an anisotropic ordered state. This ordered state could be either a liquid-crystalline phase or a dispersion of microcrystals in fluid CE. The enthalpies of melting the CE in inclusions are consistent with the latter possibility because the enthalpies are greater than the ~1 cal/g associated with melting CE liquid crystals. A limitation of the DSC approach is that some cooling of the sample below 37 °C is required. Nonetheless, the thermal data indicate either that the CE inclusions from J774 cells are partially crystalline in situ or that they are able to crystallize very readily. The ease of this crystallization is evident from the fact that when isolated inclusions are first melted, cooled quickly to room temperature, and then reheated, the enthalpy absorbed in the second scan indicates that some crystalline CE is being melted.

There are several factors which might complicate the direct application of the phase diagram presented in Figure 6 to the prediction of the physical state of CE inclusions in cells.

(1) Cholesteryl oleate and cholesteryl palmitate are the principal constituents of CE inclusions from J774 cells, but the composition of intact inclusions is more complex, so the other minor components could affect the phase behavior summarized in Figure 6. Triglycerides are known to abolish the smectic and cholesteric liquid-crystalline phases of CE at concentrations below 10% (Lundberg, 1976; Croll et al., 1985). The colligative effects due to triglycerides and other lipid components present in the inclusions are probably responsible for the fact that the two transitions observed for J774 inclusions (Figure 3A) occur at lower temperatures than they do for a 50/50 binary mixture of cholesteryl oleate/cholesteryl palmitate (Figure 5C).

(2) The cholesteryl oleate and cholesteryl palmitate were mixed in bulk to obtain the phase diagram depicted in Figure 6 whereas the CE in inclusions is dispersed as 1–2-μm diameter droplets in an aqueous medium. Phospholipid and protein are presumed to form a monolayer around a lipophilic core containing the CE and other lipids. Due to the small particle size, the physical domain of the lipid within the inclusions is more constrained than that of bulk lipid. In particles the size of human LDL (~200-Å diameter), boundary effects perturb the packing of CE molecules in the core so that they form a relatively disordered smectic phase (Armitage et al., 1976; Deckelbaum et al., 1977). However, the CE core of inclusions is 2 orders of magnitude larger than the CE core of LDL, so the boundary effects on molecular packing will be relatively minor. Indeed, it has been shown that in 1-μm-diameter particles, the size has negligible effects on the thermal transitions (Armitage et al., 1976). Thus, the equilibrium mixing and phase behavior of the CE in the core of inclusions should be the same as their behavior in a bulk phase.

(3) The influence of thermal history on the DSC behavior of inclusions and isolated CE indicates that kinetic effects can be important. The fact that CE in cells are dispersed in 1–2-μm diameter droplets is extremely significant for the metastability of liquid-crystal CE phases in inclusions (Lundberg, 1975). The rate of crystallization of CE extracted from inclusions and maintained in the bulk phase below the usual crystal melting temperature (i.e., in a supercooled state) is slow (cf. Figure 3C and Figure 4B). Supercooled CE present as a dispersion of 1-μm droplets in water will remain in metastable liquid-crystal phases even longer because the probability of nucleation within individual droplets is reduced. The reduced probability arises because the first step in the crystallization of CE most likely involves heterogeneous nucleation, and the probability of catalytic impurity being found in any droplet is much less than in a continuous bulk phase. These effects have been demonstrated in triglyceride oil-in-water emulsions where the oil can be supercooled to a much greater degree than it can in the bulk phase (Phipps, 1964).

The rate of crystallization increases with the degree of supercooling when crystallization is initiated by either hetero-

geneous or homogeneous nucleation (Adamson, 1982). At 37 °C, cholesteryl palmitate rich mixtures of cholesteryl oleate and cholesteryl palmitate in the liquid-crystal phase will be supercooled much more than cholesteryl oleate rich mixtures (Figure 6), so the cholesteryl palmitate rich liquid-crystal phases will be less stable with respect to crystallization than their cholesteryl oleate rich counterparts at the same temperature. It follows that the likelihood of microcrystalline domains forming in inclusions decreases as the content of unsaturated cholesteryl oleate rises. Consistent with this, we have reported earlier (Glick et al., 1983) that the inclusions from rat Fu5AH hepatoma cells exist in a smectic liquid-crystal phase. Unlike our present experience with J774 macrophage inclusions, where DSC indicates some crystallization of the CE, crystal formation was not evident in the hepatoma inclusions where the cholesteryl oleate/cholesteryl palmitate ratio is 1.7. In order to define the exact nature of the ordered structure which exists in inclusions in the cytoplasm of J774 cells, it will be necessary to define the metastability of the physical state of the CE. This will necessitate understanding how the minor components of inclusions, the procedures used to isolate inclusions and study them by DSC, and inclusion particle size influence the ability of CE molecules to crystallize. If the time taken for crystallization to occur is long compared to the turnover time of the CE in inclusions (Brown et al., 1980), then presumably CE liquid-crystal states in living cells could be metastable indefinitely. The current analysis suggests that in the case of J774 inclusions, microcrystals of cholesteryl palmitate exist. Within individual droplets, the microcrystals are suspended in a fluid CE phase which is bounded by a phospholipid/protein monolayer. The fluid cholesteryl oleate rich phase could be either a metastable liquid-crystal phase or a metastable isotropic liquid. The liquid-crystal phase would presumably be smectic because low levels of triglyceride destabilize the cholesteric phase (Lundberg, 1976).

ACKNOWLEDGMENTS

We thank Dr. Donald Small (Boston University) for valuable discussion.

Registry No. CO, 303-43-5; CP, 601-34-3; cholesterol, 57-88-5; cholesteryl linoleate, 604-33-1; cholesteryl myristate, 1989-52-2; cholesteryl palmitoleate, 16711-66-3; cholesteryl stearate, 35602-69-8.

REFERENCES

Adamson, A. W. (1982) *Physical Chemistry of Surfaces*, 4th ed., pp 319–331, Wiley-Interscience, New York.

Adelman, S. J., Glick, J. M., Phillips, M. C., & Rothblat, G. H. (1984) *J. Biol. Chem. 259*, 13844–13850.

Armitage, D., Deckelbaum, R. J., Shipley, G. G., & Small, D. M. (1977) *Mol. Cryst. Liq. Cryst. 42*, 203–214.

Bligh, E. G., & Dyer, W. J. (1959) *Can. J. Biochem. Physiol. 37*, 911–917.

Brown, M. S., & Goldstein, J. L. (1983) *Annu. Rev. Biochem. 52*, 223–261.

Brown, M. S., Ho, Y. K., & Goldstein, J. L. (1980) *J. Biol. Chem. 255*, 9344–9352.

Croll, D. H., Small, D. M., & Hamilton, J. A. (1985) *Biochemistry 24*, 7971–7980.

Deckelbaum, R. J., Shipley, G. G., & Small, D. M. (1977) *J. Biol. Chem. 252*, 744–754.

Dulbecco, R., & Vogt, M. (1954) *J. Exp. Med. 99*, 167–182.

Glick, J. M., Adelman, S. J., Phillips, M. C., & Rothblat, G. H. (1983) *J. Biol. Chem. 258*, 13425–13430.

Glick, J. M., Adelman, S. J., & Rothblat, G. H. (1987) *Atherosclerosis (Shannon, Irel.) 64*, 223–230.

Goldstein, J. L., Ho, Y. K., Basu, S. K., & Brown, M. S. (1979) *Proc. Natl. Acad. Sci. U.S.A. 76*, 333–337.

Hata, Y., Hower, J., & Insull, W., Jr. (1974) *Am. J. Pathol. 75*, 423–456.

Hatch, F. T., & Lees, R. S. (1968) *Adv. Lipid Res. 6*, 1–68.

Hoff, H. F., & Gaubatz, J. W. (1982) *Atherosclerosis (Shannon, Irel.) 42*, 273–297.

Johnson, W. J., Bamberger, M. J., Latta, R. A., Rapp, P. E., Phillips, M. C., & Rothblat, G. H. (1986) *J. Biol. Chem. 261*, 5766–5776.

Kanazawa, T., Izawa, M., Kaneko, H., Onodera, K., Metoki, H., Oike, Y., & Senyang, L. (1987) *Exp. Mol. Pathol. 47*, 166–174.

Katz, S. S., Shipley, G. G., & Small, D. M. (1976) *J. Clin. Invest. 58*, 200–211.

Lundberg, B. (1975) *Chem. Phys. Lipids 14*, 309–312.

Lundberg, B. (1976) *Acta Chem. Scand., Ser. B B30*, 150–156.

Lundberg, B. (1985) *Atherosclerosis (Shannon, Irel.) 56*, 93–110.

Markwell, M. K., Haas, S. M., Bieber, L., & Tolbert, N. (1978) *Anal. Biochem. 87*, 206–210.

McCloskey, H. M., Rothblat, G. H., & Glick, J. M. (1987) *Biochim. Biophys. Acta 92*, 320–332.

Morrison, W. R., & Smith, L. M. (1964) *J. Lipid Res. 5*, 600–608.

Noble, R. P. (1968) *J. Lipid Res. 9*, 693–700.

Phipps, L. W. (1964) *Trans. Faraday Soc. 60*, 1873–1883.

Ralph, P., Prichard, J., & Cohn, M. (1975) *J. Immunol. 114*, 898–905.

Rosenfeld, M. E., Tsukada, T., Chait, A., Bierman, E. L., Gown, A. M., & Ross, R. (1987) *Arteriosclerosis (Dallas) 7*, 24–34.

Rothblat, G. H. (1974) *Lipids 9*, 526–535.

Rothblat, G. H., Rosen, J. M., Insull, W., Jr., Yau, A. O., & Small, D. M. (1977) *Exp. Mol. Pathol. 26*, 318–324.

Small, D. M. (1986) *Handb. Lipid Res. 4*, 395–473.

Small, D. M., & Shipley, G. G. (1974) *Science (Washington, D.C.) 185*, 222–229.

Sokoloff, L., & Rothblat, G. H. (1972) *Biochim. Biophys. Acta 280*, 172–181.

Wolfbauer, G., Glick, J. M., Minor, L. K., & Rothblat, G. H. (1986) *Proc. Natl. Acad. Sci. U.S.A. 83*, 7760–7764.